

University of Wollongong - Research Online

Thesis Collection

Title: Electronic and Optical Properties of Graphene

Author: Anthony Wright

Year: 2010

Repository DOI:

Copyright Warning

You may print or download ONE copy of this document for the purpose of your own research or study. The University does not authorise you to copy, communicate or otherwise make available electronically to any other person any copyright material contained on this site.

You are reminded of the following: This work is copyright. Apart from any use permitted under the Copyright Act 1968, no part of this work may be reproduced by any process, nor may any other exclusive right be exercised, without the permission of the author. Copyright owners are entitled to take legal action against persons who infringe their copyright. A reproduction of material that is protected by copyright may be a copyright infringement. A court may impose penalties and award damages in relation to offences and infringements relating to copyright material.

Higher penalties may apply, and higher damages may be awarded, for offences and infringements involving the conversion of material into digital or electronic form.

Unless otherwise indicated, the views expressed in this thesis are those of the author and do not necessarily represent the views of the University of Wollongong.

Research Online is the open access repository for the University of Wollongong. For further information contact the UOW Library: research-pubs@uow.edu.au

2010

Electronic and Optical Properties of Graphene

Anthony Wright
University Of Wollongong

Follow this and additional works at: <https://ro.uow.edu.au/theses>

University of Wollongong

Copyright Warning

You may print or download ONE copy of this document for the purpose of your own research or study. The University does not authorise you to copy, communicate or otherwise make available electronically to any other person any copyright material contained on this site.

You are reminded of the following: This work is copyright. Apart from any use permitted under the Copyright Act 1968, no part of this work may be reproduced by any process, nor may any other exclusive right be exercised, without the permission of the author. Copyright owners are entitled to take legal action against persons who infringe their copyright. A reproduction of material that is protected by copyright may be a copyright infringement. A court may impose penalties and award damages in relation to offences and infringements relating to copyright material.

Higher penalties may apply, and higher damages may be awarded, for offences and infringements involving the conversion of material into digital or electronic form.

Unless otherwise indicated, the views expressed in this thesis are those of the author and do not necessarily represent the views of the University of Wollongong.

Recommended Citation

Wright, Anthony, Electronic and Optical Properties of Graphene, Doctor of Philosophy thesis, School of Engineering Physics, University of Wollongong, 2010. <https://ro.uow.edu.au/theses/3123>

NOTE

This online version of the thesis may have different page formatting and pagination from the paper copy held in the University of Wollongong Library.

UNIVERSITY OF WOLLONGONG

COPYRIGHT WARNING

You may print or download ONE copy of this document for the purpose of your own research or study. The University does not authorise you to copy, communicate or otherwise make available electronically to any other person any copyright material contained on this site. You are reminded of the following:

Copyright owners are entitled to take legal action against persons who infringe their copyright. A reproduction of material that is protected by copyright may be a copyright infringement. A court may impose penalties and award damages in relation to offences and infringements relating to copyright material. Higher penalties may apply, and higher damages may be awarded, for offences and infringements involving the conversion of material into digital or electronic form.

Electronic and Optical Properties of Graphene



Anthony Wright

University of Wollongong

A thesis submitted for the degree of

Doctor of Philosophy

Certification

I, Anthony R. Wright, declare that this thesis, submitted in partial fulfilment of the requirements for the award of Doctor of Philosophy, in the School of Engineering Physics, University of Wollongong, is wholly my own work unless otherwise referenced or acknowledged. The document has not been submitted for qualifications at any other academic institution.

Anthony R. Wright

Contents

| | |
|--|-------------|
| Certification | i |
| List of Figures | iv |
| Dedication | xiii |
| List of Publications | xvi |
| Acknowledgements | xix |
| Introduction | 1 |
| 1 Electronic Properties of Graphene | 16 |
| 1.1 Single Layer Graphene (SLG) | 18 |
| 1.1.1 Full Energy Description | 19 |
| 1.1.2 Low Energy Approximation | 21 |
| 1.2 Bilayer Graphene (BLG) | 23 |
| 1.3 Graphene Nanoribbons (GNRs) | 26 |
| 1.4 Bilayer Graphene Nanoribbons (BLGNRs) | 30 |
| 1.5 Stretched Single Layer Graphene | 34 |
| 1.6 Conclusion | 38 |
| 2 Dielectric Properties of Graphene Systems | 40 |
| 2.1 Dielectric Function | 40 |
| 2.2 Collective Excitation Spectra of Armchair Graphene Nanoribbons | 43 |

| | | |
|----------|---|------------|
| 3 | Optical Conductivity of Graphene | 49 |
| 3.1 | Single Layer Graphene | 51 |
| 3.2 | Bilayer Graphene | 52 |
| 3.3 | Graphene Nanoribbons | 59 |
| 3.4 | Layered Graphene Nanoribbons | 60 |
| 3.5 | Stretched Graphene | 67 |
| 3.6 | Conclusions | 72 |
| 4 | Nonlinear Optical Conductivity of Graphene | 73 |
| 4.1 | Formalism | 73 |
| 4.2 | Results | 75 |
| 4.2.1 | Temperature Dependence of Results | 82 |
| 5 | High Frequency Conductivity of Graphene | 88 |
| 5.1 | Phonon Spectrum | 89 |
| 5.2 | Many Particle Formalism | 91 |
| 5.3 | Momentum Frequency Summation (ξ_l) | 95 |
| 5.3.1 | Diagrams two and three | 96 |
| 5.4 | Form Factor Determination | 99 |
| 5.5 | Momentum Transfer Summations (α_m) | 101 |
| 5.6 | Results and Discussions | 102 |
| 5.7 | Conclusion | 108 |
| | Conclusion | 109 |
| | Bibliography | 112 |

List of Figures

| | | |
|---|---|---|
| 1 | The fermions in graphene are described by the conical massless Dirac dispersion which is a low energy manifestation of an ultra-relativistic equivalent dispersion. The fermions in bilayer graphene have no known equivalent, and can be described as massive chiral fermions with a symmetrical bandstructure. | 5 |
| 2 | The proposed setup to demonstrate the Klein paradox. An incoming Dirac Fermion hits a finite potential well of magnitude V_0 and width D . The transmission is calculated as usual in elementary quantum mechanics by demanding the continuity of the wavefunctions. Figure from reference (1) | 6 |
| 3 | The transmission results from equation 7 for different values of V_0 , where $D = 110\text{nm}$ (top), and $D = 50\text{nm}$ (bottom). Aside from normal incidence there are potentially other points of absolute transmission as well. This absolute transmission is a manifestation of the Klein paradox. Figure from reference (1) | 7 |
| 4 | Laughlin's proposed experiment to probe the quantum Hall effect in graphene. He suggested a carbon nanotube type configuration with a magnetic field passing through the surface of the tube, and a current passing circumferentially around the tube such that there is a flux ϕ down the axis of the tube, and a Hall voltage V_H is induced perpendicular to the field. Figure from reference (1) . . . | 9 |

LIST OF FIGURES

| | | |
|-----|---|----|
| 5 | The measurement of the anomalous integer Quantum Hall Effect for graphene. As reasoned by several authors, there is no Hall plateau at $N = 0$. The peak of the blue line at $n = 0$ shows that there is a Landau level when the chemical potential at the neutrality point which draws states equally from the conduction and valence bands. Figure from reference (1) | 10 |
| 6 | The measurement of the universal conductivity of graphene performed by Nair et al and published in Science magazine ???. Amazingly, the universal conductivity is directly proportional to the fine structure constant, and provides an alternative (albeit less accurate) method for determining it. | 11 |
| 7 | The optical conductivity of graphene outside the Dirac regime contains significant structure which is lost when confined to the linear approximation to the Hamiltonian. The peak corresponds to a van-Hove singularity in the density of states. The full energetic range is $0 < \hbar\omega < 9\text{eV}$. The Dirac formalism is roughly applicable up to $\approx 1\text{eV}$ | 12 |
| 1.1 | Single layer graphene contains two atoms per unit cell, generally denoted by A and B. The first nearest neighbour vectors are shown ($\hat{\delta}_i$), as well as the lattice vectors (\mathbf{a}_{\pm}). The electronic structure is investigated via the tight binding approximation. | 18 |
| 1.2 | The three interlayer terms included in the BLG Hamiltonian, as well as the next nearest neighbour coupling term. γ_2 and γ_3 differ in that they connect, respectively, different and equivalent points in the SLG Brillouin Zone. Whilst γ_1 and γ_2 both represent coupling between different sites in the Brillouin zone, γ_1 is a directly vertical transition, and so the overlap of the wavefunctions is much larger ($\approx 3\times$ larger) | 24 |
| 1.3 | The k_x dependence of the bandstructure near the K/K' points with all coupling terms included. The two arrows show the approximately constant (at low energies) gap between similar bands. | 25 |

| | | |
|-----|---|----|
| 1.4 | The k_x dependence of the two inner bands near the K/K' points zoomed right in to see the effects of γ_2 and γ_3 . The NNN interaction has shifted these features well below the Fermi level. γ_2 causes the second dirac point to emerge, and γ_3 causes one of the two Dirac points to occur at a lower energy. | 25 |
| 1.5 | The two most typical GNRs are $q = 0$, corresponding to zig-zag ribbons, and $q = 1$, corresponding to armchair ribbons. The elegance of Ezawa's construction is the simplicity of constructing infinite ribbons by placing consecutive stacks of hexagon layers on top of each other, offset by q hexagons. The zig-zag and armchair edges can be readily seen. These are what determine the unique electronic properties of each class of ribbon. The index p essentially determines the width, and does not alter the electronic properties <i>as much</i> as q | 26 |
| 1.6 | (a) A typical zig-zag nanoribbon bandstructure ($p = 2$). Note that at the brillouin zone edges the energy gap becomes zero. This is the case for all ZZ-GNRs. The linear Dirac dispersion is, however, not present, in these structures. (b) A typical armchair nanoribbon bandstructure ($p = 2$). The low energy linear Dirac dispersion occurs in armchair ribbons where $p + 1 \subset N$. For all other AC-GNRs, there is a small band gap. (c) A $\langle 3, 3 \rangle$ chiral GNR. A small number of GNRs with $q > 1$ have a linear Dirac-like dispersion with no energy gap, but in general this will not be the case, and the bandgaps and curvature of the bands will vary dramatically from ribbon to ribbon. | 28 |
| 1.7 | A selection of armchair and zig-zag lgnrs with the two distinct possible stacking orientations. These cause different edge sites to couple between layers in slightly different ways, leading to subtle changes in the electronic bandstructure. | 30 |

| | | |
|-----|--|----|
| 1.8 | The bandstructures for the high symmetry bilayer ribbons ($q = 0, 1$), with $p = 2$. In general, when going from a single to a bilayer ribbon, each single layer subband becomes a subband pair which are separated from each other by some amount determined by the interlayer edge state coupling. Note in particular the key differences depending on stacking orientation are at the K and Γ points. | 32 |
| 1.9 | The effect of stretching on the three nearest neighbour bond directions when F is applied along various high symmetry directions. The dotted lines in b,c and d are the regular unstretched orientations. The magnitude of F has been chosen to be very large ($F \approx 15$) to emphasise the effect of stretching, however our numerical results will only go as high as $F = 2.5$ | 36 |
| 2.1 | A hand waving approach to the screened interaction of an electronic system. The infinite sum of intermediate interactions leads to a denominator which is the RPA dielectric function of the system. | 41 |
| 2.2 | The collective excitation spectrum for Dirac armchair ($q = 1$) ribbons. The linear behaviour akin to collective excitation in metals is present for low widths, and low momentum transfers, as expected. At higher transfers and widths, the non-metallic subbands are no longer suppressed and cause the spectra to become curved. | 44 |
| 2.3 | Top: The collective excitation spectrum for non-Dirac armchair ($q = 1$) ribbons. The roton mode emerges here for $p = 18$, and for $p \geq 21$ there is a region where no excitations occur. Bottom: The frequency and wavevector dependent intensity distribution for a non-Dirac armchair (19,1) ribbon. | 45 |

| | | |
|-----|--|----|
| 2.4 | <p>The dielectric function of the armchair ribbon exhibiting a roton mode is shown here for two values of $\hbar\omega/t$. (a) is that for $\hbar\omega/t = 0.35$ which is within the roton section of the spectrum. The two excitation peaks are clearly visible. For higher energies, the imaginary part is no longer negligible, and suppresses the excitations. This is seen in (b) where $\hbar\omega/t = 1$. Note that the collective excitation peaks have been normalized by the maximum magnitude of the real and imaginary parts of ϵ.</p> | 47 |
| 3.1 | <p>The single loop diagram describing the linear optical conductivity in the absence of interactions.</p> | 50 |
| 3.2 | <p>The k_x dependence of the bandstructure near the K/K' points. The effect of the NNN coupling is to shift the Fermi level (here $\epsilon_F = 0$) off the bands-crossing points. The other noticeable effect here is that of the dominant interlayer coupling γ_1 which causes the gap of $\Delta \approx \gamma_1$ between similar bands. The red dashed arrow represents a transition which is permitted in an intrinsic bilayer calculation if NNN coupling is neglected in the model, but becomes forbidden when it is included. The black solid arrow is the opposite: a previously forbidden transition becomes allowed when NNNs are included in the model. The effect of doping is to raise or lower the Fermi level, making the inclusion of NNNs partly equivalent to doping.</p> | 57 |
| 3.3 | <p>The optical conductance (in units of $\sigma_1 = e^2/\hbar$) vs the normalized frequency $\Omega = \hbar\omega/t$ for bilayer graphene. Generally, σ_{xx} (the zigzag direction) has a larger optical response than σ_{yy} (the armchair direction). When NNN and γ_4 are neglected, and at low energies, $\sigma_{xx} = \sigma_{yy}$. This is no longer the case here, with NNNs and γ_4 included. The grey shaded area indicates the low energy region plotted in Fig.3.4.</p> | 57 |

| | | |
|-----|---|----|
| 3.4 | <p>The low energy optical conductance at two different doping levels. The blue dash-dot and black dashed lines are the optical conductance of intrinsic BLG along the x and y directions respectively. The black solid and blue dotted lines represent the optical conductance of a sample which is doped such that the chemical potential is shifted to the bands crossing point. The NNN-γ_4 coupling causes a new peak to emerge, and suppresses the previously reported one. This new peak is much larger and shifted to a lower photon energy. In a suitably doped sample, however, the $t' = 0$ (no NNN) peak has been retrieved by an effective shifting of the Fermi level. The inset shows the sensitivity of the intrinsic zig-zag peak to the Fermi energy. Δ is the bands crossing point. If the Fermi energy lies at least $0.6t'$ from the bands-crossing points (in either direction), the peak conductance lies within 15% of our result.</p> | 58 |
| 3.5 | <p>The optical conductivity for the ZZ-BLGNR (a) and the AC-BLGNR (b). The low energy activity in the bilayer ribbons is particularly significant, especially in the Dirac AC-BLGNR where the optical conductivity is approximately $150\sigma_0$. The temperature dependence of the large peak observed in all armchair bilayer ribbons is shown in the inset. The peak is robust all the way up to room temperature, decreasing rapidly to $\approx 80\sigma_0$ at $10K$ then decreasing very slowly with increasing energy.</p> | 61 |
| 3.6 | <p>The width dependence of the energy of the low-energy peak for BLGNRs with $q = [1, 4]$. The strongest peaks occur in the lowest energy gaps in the Dirac armchair ribbons. The inset shows the width dependence of the band gap for Dirac BLGNRs with strong low energy optical response. This gap eventually disappears, but in the 2D limit with no edges, it re-emerges at γ.</p> | 63 |

| | | |
|------|---|----|
| 3.7 | The p dependence of the low energy peaks for a (p,1) BLG NR. In Dirac ribbons the symmetric transitions are suppressed and the non-symmetric ones dominate. For non-Dirac ribbons the opposite is the case. Notice that the strength of the peak in the Dirac cases is constant (within the specified computational accuracy of the calculation). | 64 |
| 3.8 | The width dependence of the magnitude of the low energy peak for the ZZ-BLG NRs decreases quickly with increasing width, and then increases steadily for $p > 6$ | 65 |
| 3.9 | The stretching induced anisotropy in the longitudinal conductivity for three small pseudo force values. These correspond to bond stretching angles of $\approx 0.4, 1.2, 2$ degrees for $F = 0.5, 1.5, 2.5$ respectively. Despite the relatively small stretching angle, the induced anisotropy is as much as 10%. The angular dependence of this quantity is quite well behaved. When stretching along the zig-zag direction, the zig-zag longitudinal conductivity is increased, and similarly for stretching along the armchair direction. For stretching of $\pi/4$, the system remains isotropic. | 69 |
| 3.10 | The transverse optical conductivity as a function of stretching angle. Interestingly, even though the C_3 symmetry is broken for stretching along the high symmetry directions, the transverse conductivity remains zero. For chiral stretching this is not the case. Maximum stretching is reached for the longitudinally isotropic value of $\phi = \pi/4$ | 70 |
| 3.11 | The transverse (Hall) conductivity for $\phi = 45^\circ$ and $F = 2.5$. The transverse conductivity reaches a maximum of $\approx 0.85\sigma_0$ at the high density of states saddle point $\Omega = 2$ | 71 |
| 4.1 | A schematic illustration of linear and nonlinear optical processes in intrinsic graphene. The universal conductance described by \mathbf{J}_1 . The two third order terms $\mathbf{J}_3(\omega)$ and $\mathbf{J}_3(3\omega)$ are shown in blue and green colour. The latter is a frequency tripling term which is the dominant nonlinear current. | 75 |

LIST OF FIGURES

| | | |
|-----|--|----|
| 4.2 | The frequency dependent nonlinear current. Both the single frequency and frequency tripling terms decrease as ω^{-4} , and also with increasing temperature. At low frequencies, low temperatures, and sufficiently high field strengths, the nonlinear terms will contribute to the optical conductance of graphene. In particular, the single frequency term will abolish the universality of the ‘universal conductance’ under the right conditions. | 85 |
| 4.3 | (a) The difference between the critical fields at 0K and 300K as a function of frequency (ie. $\Delta E_c = E_c(0K) - E_c(300K)$). There is a maximum discrepancy for each nonlinear contribution which indicates the frequency where thermal effects are most significant. (b) The temperature dependence of the critical field strength at fixed frequency. At low temperatures the single frequency nonlinear current dominates over the frequency tripling term. At $\approx 180K$ however, the situation is reversed such that at room temperature, the frequency tripling term is the dominant nonlinear contribution. | 87 |
| 5.1 | The fourth nearest neighbours for graphene. We include up to fourth nearest neighbours so that the bond-bending effect of the third and fourth neighbours will be included. | 90 |
| 5.2 | The phonon spectrum of graphene obtained using the fourth nearest neighbour force constant tensor method. | 91 |
| 5.3 | The five diagrams which contribute to the high frequency correction to the optical conductivity. | 93 |
| 5.4 | The effective interaction is given by the bare phonon propagator plus an intermediate electron-phonon interaction, which causes a density fluctuation described by the electron propagator loop, followed by an effective interaction. This diagram describes the infinite sum implied by equations 5.14 & 5.16. Taking the effective interaction to be of this form is equivalent to adopting the RPA approximation. | 94 |

| | | |
|-----|---|-----|
| 5.5 | The electron-phonon scattering mediated conductivity of graphene. In (a) we present both the intraband and interband contributions. It is found that for $T > 100K$ the intraband contributions dominate. The $T = 30K$ results are shown in the inset due to their relatively small magnitude. In (b) we show the interband part which is shown to have several multi-phonon processes, but the magnitude of this contribution is relatively negligible except at very low and very high temperatures. | 105 |
| 5.6 | The temperature dependence of the magnitude of the conductivity at $\omega = \omega_{LO}/2$ (the continuum peak), and $\omega = \omega_{LO}$, (the dominant resonant peak) from figure 5.5. In (a) we show the inter- and intraband contributions together and obtain a roughly linear relationship. When plotted in log-log form (inset), we see that there is a significant ‘kink’ at $T \approx 30K$. When considering only interband transitions as in (b), both peaks display an exponential temperature dependence. | 106 |
| 5.7 | The two dominant response peaks increase in magnitude for doped samples, and are symmetric about zero doping due to electron-hole symmetry. This can be attributed to the increased availability of intraband transitions, which are the dominant mechanism. . . . | 107 |

To my beautiful wife Ally – friend, companion, comrade

Abstract

We investigate the electronic and optical properties of various one and two dimensional graphene based materials. Using the tight binding approximation, we calculate the electronic dispersions of these systems. Using Green's functions, we then evaluate the dielectric function within the random phase approximation (RPA), and the corresponding collective excitation spectrum for armchair graphene nanoribbons. We also calculate the Kubo formula-based optical conductivity of single layer graphene, bilayer graphene, graphene nanoribbons, bilayer graphene nanoribbons, and stretched graphene. For single layer graphene within the Dirac approximation we also calculate the third order nonlinear optical conductance (a nonlinear correction to the 'universal' conductivity, as well as a frequency tripling term) and finally the effect of electron-LO phonon scattering on the 'universal' conductivity at various temperatures and doping levels.

There are several results of particular interest. We predict a roton-like mode in the collective excitation spectrum of non-Dirac armchair graphene nanoribbons. We also demonstrate a two order of magnitude enhancement to the optical conductivity of an entire subclass of bilayer graphene nanoribbons in the terahertz-far infrared regime. A strong nonlinear conductance of single layer graphene under moderate field strengths at room temperature is derived. Finally, stretching induced hall optical conductivity and chirality dependent anisotropy in single layer graphene under conservative stretching conditions are predicted.

We find that the optical properties of graphene based materials are remarkably robust and highly tunable, particularly within the terahertz

to far-infrared regime. Furthermore, the prediction of a roton-like minimum in the collective excitation spectra of a subclass of armchair ribbons makes these particular graphene based materials part of an extremely small subclass of materials, and represents the opening of a potentially huge new field of fundamental research.

List of Publications

Refereed Journal Articles

1. Wright A.R., and Zhang C. “Dynamic conductivity of graphene with electron-LO-phonon interaction” Phys. Rev. B. **81**, 165413 (2010).
2. Wright A.R., Cao J.C., and Zhang C. “Enhanced optical conductivity of bilayer graphene nanoribbons in the terahertz regime” Phys. Rev. Lett. **103**, 207401 (2009).
3. Wright A.R. and Zhang C. “Stretching induced conductance anisotropy and Hall current in graphene” App. Phys. Lett. **95**, 163104 (2009), selected for the November 2, 2009 issue of Virtual Journal of Nanoscale Science & Technology.
4. Wright A. R., Xu X. G., Cao J. C., and Zhang C., “Strong nonlinear optical response of graphene in the terahertz regime”, Applied Physics Letters **95**, 072101 (2009), selected for the August 31, 2009 issue of Virtual Journal of Nanoscale Science & Technology.
5. Wright A. R., Liu F., and Zhang C., “The effect of next nearest neighbour coupling on the optical spectra in bilayer graphene” Nanotechnology **20**, 405203 (2009).
6. Liu J., Wright A. R., Zhang C. and Ma Z., “Strong terahertz conductance of graphene nanoribbons under a magnetic field”, Applied Physics Letters **93** (4), 041106, (2008).

7. Liu J., Ma Z., Wright A. R. and Zhang C., “Orbital magnetization of graphene and graphene nanoribbons”, *Journal of Applied Physics* **103**, 103711 (2008).
8. Li Z., Ma Z., Wright A.R., Zhang C., “Spin-orbit interaction enhanced polaron effect in two-dimensional semiconductors”, *Applied Physics Letters* **90**, 112103 (2007).
9. Yang C.H., Wright A.R., Gao F., Zhang C., Zeng Z., Xu W., “Two colour plasmon excitation in an electron-hole bilayer structure controlled by the spin-orbit interaction”, *Applied Physics Letters* **88**, 223102 (2006).

Submitted Manuscripts

1. Wright A.R. and Zhang C., “Roton Mode in the Collective Excitation Spectrum of Graphene Nanoribbons”, Submitted to *Physical Review Letters*.
2. Wright A.R. T. E. O’Brien, D. Beavan, and Zhang C., “Band-gap scaling and gapless insulator in semi-hydrogenated graphene”, Submitted to *Physical Review Letters*.

Refereed Conference Papers

1. Wright A.R. and Zhang C., “Strong optical absorption of bilayer graphene in THz-FIR regime”, to be published in proceedings of IRMMW’09 - Invited Talk upgraded to Keynote Presentation based on this manuscript.
2. Wright A.R. and Zhang C., “Optical absorption of bilayer graphene nanoribbons”, to be published in proceedings of CLEO-Asia ’09
3. Wright A.R., Wang G.X., Xu W., Zeng Z., and Zhang C., “The spin-orbit interaction enhanced terahertz absorption in graphene around the K point”, *Microelectronics Journal* **40**, 857 (2009).
4. Wright A.R., Liu J., Ma Z., Zeng Z., Xu W., Zhang C., “Thermodynamic properties of graphene nanoribbons under zero and quantizing magnetic fields”, *Microelectronics Journal* **40**, 716 (2009).

5. Li L.L., Xu W., Zeng Z., Wright A.R., Zhang C., Zhang J., Shi Y.L.,
“Mid-infrared absorption by short-period InAs/GaSb type II superlattices”
Microelectronics Journal **40**, 815 (2009).
6. Xu W., Zeng Z., Wright A.R., Zhang C., Zhang J., Lu T.C., “Exchange-
induced band hybridization in InAs/GaSb based type II and broken-gap
quantum well systems”, Microelectronics Journal **40**, 809 (2009).
7. Li L. L., Xu. W., Zeng Z., Wright A. R., Zhang C., Zhang J., Shi Y.
L., Lu T. C., “Terahertz band-gap in InAs/GaSb type-II superlattices”,
Microelectronics Journal **40**, 812 (2009)

Acknowledgements

When sitting alone in the office I sometimes feel very isolated. However, friendship and collaboration have been found through the following people. I am greatly indebted to my supervisor, Prof. Chao Zhang. I defy anyone to show me a better supervisor. Chao has treated me with respect and generosity. He is always available for a chat, and knows everything about everything. I have thoroughly enjoyed working with him on projects since 3rd year, and have only come to respect him more with time.

Thankyou to the rest of the faculty, particularly Dr David Martin for being a dedicated teacher who is always keen for a chat about interesting things and is always very encouraging, Dr George Takacs for being another dedicated teacher, and a good bloke who cares about more than just physics, Mr Duncan Fischer for being another good guy and role model for good teaching, and Prof. Roger Lewis for being ever encouraging and enthusiastic especially when it comes to 'Christian' matters.

Thanks to Mr Daniel Bell for being an extremely good friend throughout my university years, especially for keeping on coming back to the uni even after graduating, and especially for sticking around in Wollongong. Thanks also to Mr Pete Reeve for being a good mate who loves physics, homebrew, and most of all, Jesus.

Thanks to my family for loving and caring for me. Thanks for taking an interest in my ostensibly boring work. Thanks particularly to Mavis for the blanket for my knees.

Thankyou to my beautiful wife Ally who I love. Thankyou for growing up with me. Thanks for trying to be interested in my work. Thanks

for proof-reading everything even though it can't have been interesting. Thankyou for loving me and caring for me, even when I didn't do the same for you. And thankyou to Rose for being a beautiful ray of sunshine in this last year. It has been wonderful watching you grow up and learn to do all sorts of wonderful new things.

And most importantly thankyou to the God and Father of my Lord Jesus Christ, who has blessed me in the heavenly realms with every spiritual blessing, and will save me on the last day from my rottenness because He said he would through the death of his Son. This is more love than I know what to do with. It is for his glory that this work was undertaken.

Introduction

The field of graphene research is *huge* (1; 2; 3). Since the invention of carbon nanotubes in 1991 (4), research into hexagonally arrayed graphitic carbon systems has escalated. Despite being a simpler and more versatile system to consider theoretically, graphene's rise took place more than a decade later in 2003, when the group of Novoselov and Geim reported that they had managed to create and detect single and few layer graphite (5). Since this first seminal work was performed, publications in the field of graphene based structures has exploded.

In 1946, long before its intentional fabrication, P.R. Wallace developed the tight binding bandstructure theory of graphene and demonstrated its unusual properties (6). The motivation for this work was the extension to a superlattice which he would use to describe the properties of bulk graphite. In 2003 however, this work took on new significance, and Wallace's pioneering work turned out to be 60 years ahead of its time. 20 years after this seminal work, Slonczewski, Weiss, and McClure (SWM) developed the interlayer coupling theory for stacked graphene (7; 8). The collective work of these three was remarkably successful at the time, and again has resurfaced in the context of stacked graphene layers. Utilising the theories of Wallace and SWM, single layer graphene, bilayer graphene, graphene nanoribbons, layered graphene nanoribbons, and the curved, rolled, crumpled, rippled, stretched (and any other deformation imaginable) variations on these materials have been successfully and extensively studied over the last few years.

The focus of much of the current research on graphene structures is concerned with so-called 'Dirac fermions' (although the recent review by Geim expounds the ever growing volume of work in other areas (2)). The low energy bandstructure of graphene is conical, which immediately implies a constant density of states

(DOS), a constant group velocity akin to the behaviour of photons or neutrinos, and electron hole symmetry. The latter two have been confirmed experimentally (9). This unusual ‘massless’ low energy bandstructure makes graphene a veritable treasure-trove of never before seen properties, and also a potential low energy, solid state laboratory for experiments in relativistic quantum electrodynamics in $2 + 1$ dimensions. Therefore, since 2003 many interesting properties of graphene have been predicted and observed, such as the half-integer quantum Hall effect (9; 10), finite conductivity at zero charge-carrier concentration (9), the strong suppression of weak localization (11; 12; 13), and the prediction of almost perfect fluidity (14), to name just a few. These properties can be attributed to the linear ‘Dirac’ bandstructure, and low dimensionality, which lead to aforementioned QED-like effects, rather than particulate ones (15; 16).

There is a plethora of interesting phenomena pertaining to the unique properties of graphene based systems. They are outlined in detail in the excellent review articles available on the subject (1; 2; 3).

The ‘universal’ conductance of graphene is a remarkable ac phenomenon (17). It is a direct result of the linear energy dispersion of graphene. As already mentioned, linear subbands imply a constant density of states, but also consistent transition matrix elements, which means that for as long as the Dirac approximation is valid, the conductance is a constant. The value of the universal conductance of single layer graphene is $\sigma_0 = e^2/4\hbar$. This result is easily achieved by several methods. In particular the Kubo formula yields this result for an intrinsic system and neglecting electron-electron (or any other) interactions.

Deviations from ‘universal’ conductance have been shown to occur due to variations in geometry (18; 19), field energy (20; 21), and field intensity (22; 23). It need not be demonstrated that the effect of finite temperature on the distribution functions, as well as doping to create an effective band gap between available states, will also alter the value of σ_0 , especially at lower energies.

In fact, the optical properties of graphene based systems has become quite an active field of research. After the initial flurry of excitement that followed the demonstration of the universal conductivity at energies as high as the optical regime – a direct demonstration of the accuracy of the Dirac bandstructure – there has been increasing interest in graphene based materials for photonic applications,

as well as the realization of graphene's potential in the THz-FIR regime, which have lead to some very interesting results.

With all these predictions and observations having emerged, the optical properties of graphene based systems appear to be more significant and more versatile than perhaps previously believed. With this trend in mind we have proceeded to calculate the optical properties of various graphene based systems under different conditions. The motivation being based on the premise that the 'interesting' optical properties of graphene based systems have not yet been exhausted. As it turns out, our intuition is confirmed, and graphene-based systems produce a rich tapestry of optical properties which are often able to be tuned to one's specific needs, and are often quite unique in the broader field of the optical properties of condensed matter systems.

Our focus has been largely restricted to the THz-FIR regime. The motivation for this choice is the potential use of graphene in photonic device applications in the increasingly important THz band, and the ubiquitous infrared, which is so important for telecommunications purposes. The universal conductivity of graphene has a value of $\sigma_0 = e^2/4\hbar$, which leads to an optical absorption of $\approx 3\%$. Although a remarkably strong value for a single atomic layer system, in absolute terms this is a very weak response, which severely limits the potential applicability of graphene based systems in photonic devices. Therefore we have calculated the optical response for various graphene based systems to determine whether this response can be improved, or whether interesting effects such as anisotropy, nonlinear effects, or non-zero transverse conductivity can be obtained. These results will be presented in due course.

Before delving into the main results of the thesis, we must discuss the geometry of the different graphene systems investigated in this thesis. We will discuss their various electronic properties within the tight binding formalism. This will be the subject of chapter one. After this we will talk briefly about the dielectric properties of one particular graphene system: non-Dirac armchair graphene nanoribbons. This will be the subject of chapter two. The remaining chapters will be devoted to the optical conductance of graphene based systems. We will end with some concluding remarks.

Some Interesting Properties

Unique Dispersions

Firstly however, it may be interesting to summarize some of the more striking properties of graphene-based materials which make them so fascinating to study. The obvious starting point is the electronic dispersions of single and bi-layer graphene. These will be discussed in more detail in the next chapter, and so for now we will consider just the results. The electronic dispersion of graphene near the vertices of the hexagonal Brillouin zone (the K points), is

$$\epsilon_{s,\mathbf{k}} = s v_F |\mathbf{k}|, \quad (1)$$

Where $s = \pm$, and v_F is the Fermi velocity which is $\approx 10^6 \text{ms}^{-1}$. This conical dispersion, which is applicable up to energies of $\approx 1\text{eV}$, makes the fermions in graphene behave as massless particles like photons or neutrinos, and make the Dirac equation, rather than the Schrodinger equation, the natural formalism to use to describe the system. As already mentioned, this opens the gateway to potential “QED-in-a-lab” experiments (1), and also may well revolutionize modern electronics.

Bilayer graphene, near the K points, also has a unique band structure in materials science. The fermions in bilayer graphene can be described as massive Chiral fermions with a symmetrical bandstructure about the neutrality point. The low energy dispersion can be given by

$$\epsilon_{s,\mathbf{k}} = s v_F^2 k^2 / t_{\perp} \quad (2)$$

Where t_{\perp} site-equivalent interlayer coupling (see next chapter). The uniqueness of these two systems can be seen in the figure from the excellent recent review article by A.K. Geim (2) which has been reproduced here in figure 1

The interlayer term in bilayer graphene can be viewed as contributing a mass term to the Dirac equation in making the transition from one to two layers.

With these dispersions in mind, let’s look at a few of the interesting consequences of these unique materials.

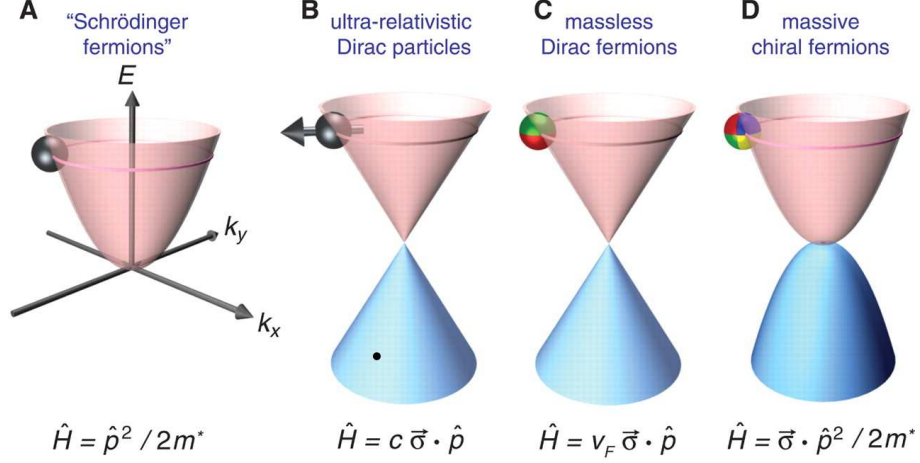


Figure 1: The fermions in graphene are described by the conical massless Dirac dispersion which is a low energy manifestation of an ultra-relativistic equivalent dispersion. The fermions in bilayer graphene have no known equivalent, and can be described as massive chiral fermions with a symmetrical bandstructure.

The Klein Paradox

An elegant example of the unusual chiral properties of graphene is in the derivation of the Klein paradox (16; 24). We first note that the wavefunction for Dirac fermions in graphene can be given by

$$\psi(\mathbf{k}) = \frac{1}{\sqrt{2}} \begin{pmatrix} 1 \\ \pm e^{i\phi(\mathbf{k})} \end{pmatrix} \quad (3)$$

Where $\phi(\mathbf{k}) = \tan^{-1} k_y/k_x$. We now consider scattering by a finite potential well of magnitude V_0 and width D , as shown in figure 2. There are thus three regions as marked in the figure. In region I, we have

$$\psi_I(\mathbf{r}) = \frac{1}{\sqrt{2}} \begin{pmatrix} 1 \\ s e^{i\phi(\mathbf{k})} \end{pmatrix} e^{i(k_x x + k_y y)} + \frac{r}{\sqrt{2}} \begin{pmatrix} 1 \\ s e^{i(\pi - \phi(\mathbf{k}))} \end{pmatrix} e^{i(-k_x x + k_y y)} \quad (4)$$

Which has a right and left moving component, where $s = \pm 1$, and in polar coordinates, and considering fermions with Fermi momentum k_F , we have $k_y = k_F \sin \phi(\mathbf{k})$ and $k_x = k_F \cos \phi(\mathbf{k})$. In region II

$$\psi_{II}(\mathbf{r}) = \frac{a}{\sqrt{2}} \begin{pmatrix} 1 \\ s' e^{i\theta} \end{pmatrix} e^{i(q_x x + k_y y)} + \frac{b}{\sqrt{2}} \begin{pmatrix} 1 \\ s' e^{i(\pi - \theta)} \end{pmatrix} e^{i(-q_x x + k_y y)} \quad (5)$$

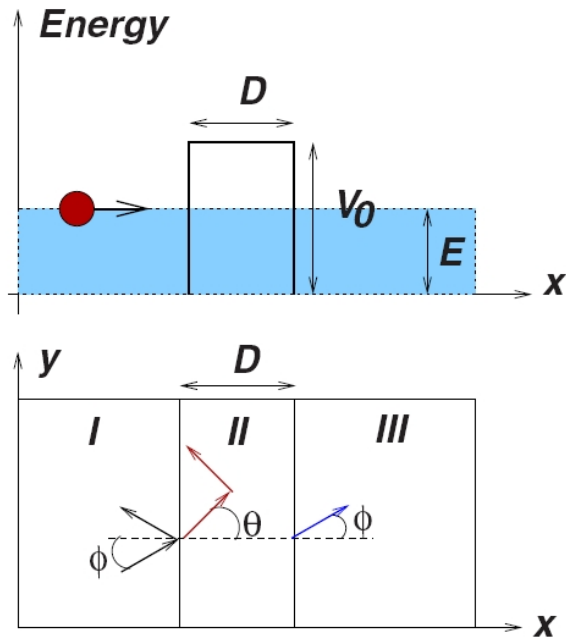


Figure 2: The proposed setup to demonstrate the Klein paradox. An incoming Dirac Fermion hits a finite potential well of magnitude V_0 and width D . The transmission is calculated as usual in elementary quantum mechanics by demanding the continuity of the wavefunctions. Figure from reference (1)

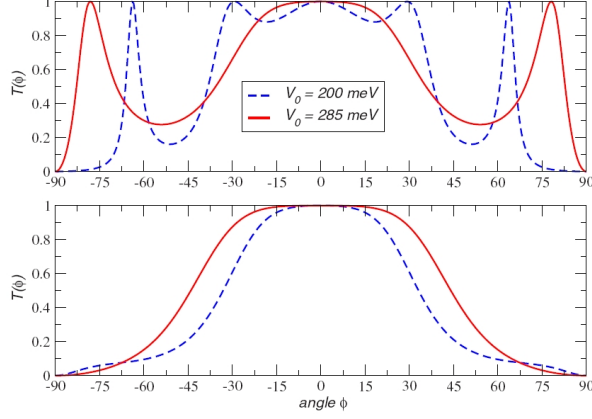


Figure 3: The transmission results from equation 7 for different values of V_0 , where $D = 110\text{nm}$ (top), and $D = 50\text{nm}$ (bottom). Aside from normal incidence there are potentially other points of absolute transmission as well. This absolute transmission is a manifestation of the Klein paradox. Figure from reference (1)

Where $\theta = \tan^{-1}(ky/qx)$, and $q_x = \sqrt{(V_0 - E)^2/(v_F)^2 - k_y^2}$, and for region III we have only a right moving component

$$\psi_{III}(\mathbf{r}) = \frac{t}{\sqrt{2}} \begin{pmatrix} 1 \\ s e^{i\phi(\mathbf{k})} \end{pmatrix} e^{i(k_x x + k_y y)} \quad (6)$$

Where $s = \text{sgn}(E)$ and $s' = \text{sgn}(E - V_0)$. According to the standard prescription, the coefficients of the wavefunctions must be determined such that continuity is preserved at the boundaries $x = 0, D$, but the derivative need not be matched in this case, unlike with the Schrodinger equation. The transmission as a function of incident angle is $T(\phi) = tt^*$, and is given by

$$T(\phi) = \frac{\cos^2 \theta \cos^2 \phi}{(\cos(Dq_x) \cos \phi \cos \theta)^2 + \sin^2(Dq_x)(1 - ss' \sin \phi \sin \theta)^2} \quad (7)$$

What is unusual about this result is that for $Dq_x = n\pi$, the barrier becomes completely transparent ($T(\phi) = 1$), which includes normal incidence ($\phi \rightarrow 0$). This is the Klein paradox, and is unique for relativistic electrons. Some nice results are reported in figure 3, where, depending on the value of V_0 , there are several points with complete transmission. This unusual behaviour is discussed in some detail in reference (1), and most of the discussion up to here has followed this reference closely.

Anomalous Integer Quantum Hall Effect

The components of the resistivity and conductivity tensors are given by

$$\begin{aligned}\rho_{xx} &= \frac{\sigma_{xx}}{\sigma_{xx}^2 + \sigma_{xy}^2} \\ \rho_{xy} &= \frac{\sigma_{xy}}{\sigma_{xx}^2 + \sigma_{xy}^2}\end{aligned}\tag{8}$$

Where σ_{xx} is the longitudinal conductivity and σ_{xy} is the Hall conductivity. When the chemical potential is inside a region of localized states, there is no longitudinal component to the conductivity. However, when the chemical potential crosses a Landau level, it is in a region of de-localized states, and $\sigma_{xx} \neq 0$, and σ_{xy} varies continuously. Imagine an experimental setup of (essentially) a carbon nanotube as proposed by Laughlin (25), and shown in figure 4. A magnetic field passes normally through the surface of the tube, and a current passes circumferentially around the loop. From the Lorentz force, the magnetic field induces a Hall voltage perpendicular to both the field and current. There is thus a magnetic flux travelling down the tube. The current is given by

$$I = c \frac{\partial E}{\partial \phi}\tag{9}$$

Where E is the total energy of the system, and ϕ is the flux. The localized states do not respond to changes in ϕ , only the delocalized ones. Imagine we now changed the flux by a single flux quantum $\Delta\phi = hc/e$. During the change of flux, an integer number of states enter the cylinder at one edge and leave at the opposite edge.

In general, due to the four fold degeneracy of the system (two equivalent K points, and assuming spin degeneracy), when the flux changes by a single quantum, the change in energy is $\pm 4NeV_H$ where V_H is the induced Hall voltage, and the \pm comes from whether they are holes or electrons. However what happens when the chemical potential is at exactly half filling – the Dirac point? According to our reasoning, there would be a Hall plateau at this level with $\sigma_{xy} = 0$. However this cannot be the case because there is a Landau level at this point, and as we stated before this rules out the plateau due to the presence of extended states.

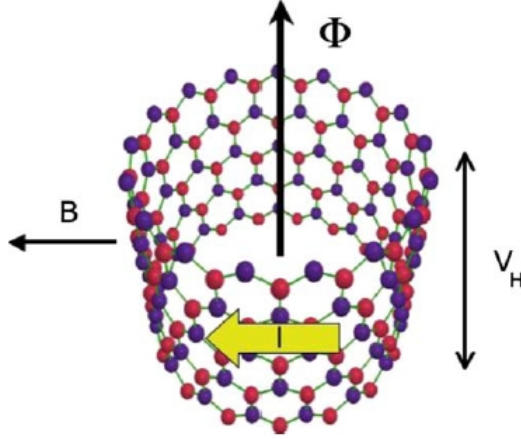


Figure 4: Laughlin’s proposed experiment to probe the quantum Hall effect in graphene. He suggested a carbon nanotube type configuration with a magnetic field passing through the surface of the tube, and a current passing circumferentially around the tube such that there is a flux ϕ down the axis of the tube, and a Hall voltage V_H is induced perpendicular to the field. Figure from reference (1)

This conundrum has been tackled by several authors, and has a rather simple explanation which is very neatly and simply explained by Castro Neto et al in reference (1): “because of the presence of the zero mode that is shared by the two Dirac points, there are exactly $2(2N + 1)$ occupied states that are transferred from one edge to another. Hence, the change in energy is $\delta E = \pm 2(2N + 1)eV_H$ for a change of flux of hc/e . Therefore, the Hall conductivity is

$$\sigma_{xy} = \frac{1}{V_H} = \frac{c\delta E}{V_H\delta\phi} = \pm 2(2N + 1)\frac{e^2}{h} \quad (10)$$

Without any Hall plateua at $N = 0$ ”!

This phenomenal and yet elegantly simple result has been realised experimentally, as shown in figure 5.

Universal Conductivity

The universal conductivity of graphene is an elegant and remarkably simple result, which shows the peculiarity of the Dirac bandstructure. We shall calculate the

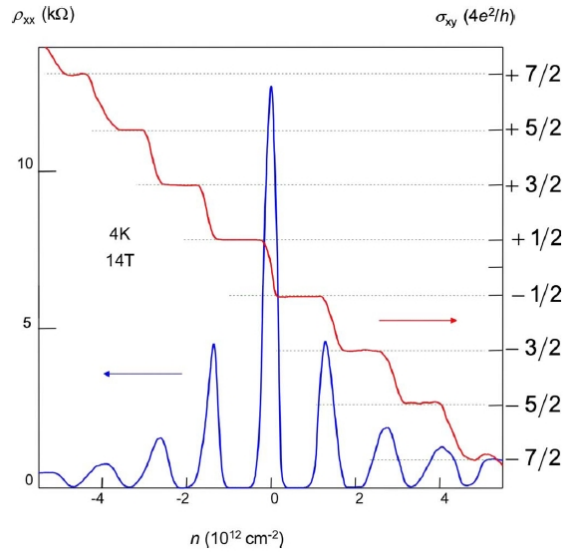


Figure 5: The measurement of the anomalous integer Quantum Hall Effect for graphene. As reasoned by several authors, there is no Hall plateau at $N = 0$. The peak of the blue line at $n = 0$ shows that there is a Landau level when the chemical potential at the neutrality point which draws states equally from the conduction and valence bands. Figure from reference (1)

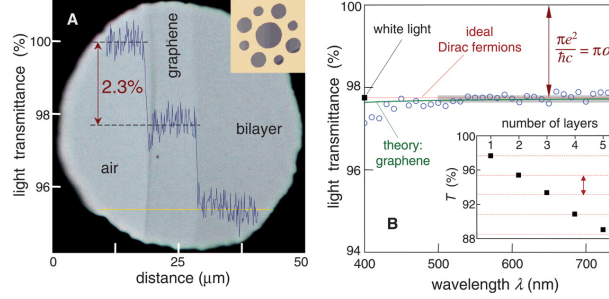


Figure 6: The measurement of the universal conductivity of graphene performed by Nair et al and published in Science magazine ???. Amazingly, the universal conductivity is directly proportional to the fine structure constant, and provides an alternative (albeit less accurate) method for determining it.

universal conductivity of graphene using the time dependent Schrodinger equation in chapter 4, but here shall reproduce the most common derivation which uses linear response theory, namely the Kubo Formula for optical conductivity. This formula will be used extensively in chapters 3 and 5, and so will be properly introduced later. For now however, we need the wavefunctions, corresponding energy levels, and the Kubo Formula. The energy levels have already been presented. The wavefunctions within the Dirac regime are

$$\langle \mathbf{k}, s | = \frac{1}{\sqrt{2}} (1 \quad s(k_x + ik_y)/k) = \frac{1}{\sqrt{2}} (1 \quad se^{i \tan^{-1}(ky/kx)}) \quad (11)$$

And the Kubo formula is

$$\sigma_{\nu, \kappa}(\omega) = \frac{1}{\omega} \int_0^\infty dt e^{i\omega t} \langle [J_\nu(t), J_\kappa(0)] \rangle \quad (12)$$

Where $\hat{v}_\mu = \partial \hat{H} / \partial k_\mu$ is the velocity operator with $\mu = x, y$. Due to the linear dispersion, the velocity operator takes on off diagonal constant values. This leads to the particularly simple result (including only interband transitions)

$$\langle \mathbf{k}, s | \hat{v} | \mathbf{k}, -s \rangle = \frac{k_x}{k^2} \quad (13)$$

We also mention in passing the breakdown of the universal conductivity with increasing energies. As mentioned earlier, the massless Dirac bandstructure quoted for single layer graphene holds up to $|\epsilon| \approx 1\text{eV}$. Moving outside of

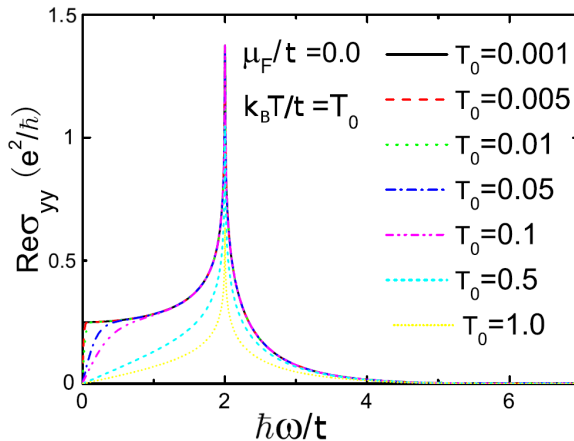


Figure 7: The optical conductivity of graphene outside the Dirac regime contains significant structure which is lost when confined to the linear approximation to the Hamiltonian. The peak corresponds to a van-Hove singularity in the density of states. The full energetic range is $0 < \hbar\omega < 9\text{eV}$. The Dirac formalism is roughly applicable up to $\approx 1\text{eV}$.

this ‘Dirac regime’, one can compute the optical conductivity after expanding the Hamiltonian to second order in momentum (21), or perform no expansions at all and proceed numerically with the full dispersion relation (20). We choose to quote the latter because this work was done within the same group as the other works in this thesis, because it was published first of the two, and finally because it is the most robust tight binding calculation performed to date (at the expense, of course, of obtaining closed form analytic results). In figure 7 we present the optical conductivity of single layer graphene over the full relevant energy range. It can be seen from this figure at what energies the Dirac approximation is appropriate in calculating the universal conductivity. For energies outside this range however, we can see that there is a peak, corresponding to a van-Hove singularity in the density of states of graphene which in turn corresponds to a saddle point in the bandstructure, followed by a gradually diminishing response for higher energies.

The unusual properties mentioned here are just a few examples of the many interesting properties of graphene based materials. The literature on graphene, despite its relatively young age, is enormous, and it is almost impossible for one

to keep abreast of the rapid progress that this field is currently undergoing. This makes graphene an exciting field to be involved in. As experimental techniques develop, one would expect that even more unexpected properties will arise with time.

Current Status and Motivation

A final word before delving into the results of this thesis. Graphene research can be, in my opinion, summarised by two major motivations: “The universe in a Helium droplet”, and “Moore’s Law”.

The former is a broad approach to condensed matter that summarises one of the most interesting aspects of modern condensed matter theory, and indeed, all of physics (and is also the title of a book by Volovik ??). As mentioned above, graphene may serve to investigate certain aspects of relativistic QED. This is not the only area where graphene research may further fundamental physics. There is a lot of interest in graphene as a quantum Hall system. The observation of fractional statistics and non-abelian quasi-particles has so far remained elusive. Quantum Hall systems are the most likely candidate systems where these are expected to be observed. Graphene may play a major role in this in the future. The quantum spin Hall effect was initially proposed for a graphene system (26), though unfortunately the intrinsic spin splitting of graphene may be too small for this proposal to be realised for graphene. Nevertheless, this has opened the door to a new class of topological insulators which are expected to be realised in other systems that can be tuned to have the same Dirac dispersions but with much larger spin-splitting. Graphene provides a solid-state laboratory with relativistic massless particles, and oddly behaved massive chiral Fermions with which we can tinker. Within the exciting field of emergent phenomena and the topological states of matter, graphene promises to provide some interesting predictions for fundamental physics.

The question of fundamental physics arising from emergent phenomena is the motivation behind the results of chapter 2 of this thesis. We calculated the collective excitation spectrum of non-Dirac armchair graphene nanoribbons and found that these materials produced plasmons with a non-propagating roton

minimum as their lowest energy excitation. This unusual result may uncover some interesting outstanding questions concerning rotons, 1D vortices, and bulk-edge coupling: questions of considerable import in the fields of Quantum Hall systems and topological states of matter. Interestingly, the only other material to display such a collective mode in the absence of an external magnetic field is the apparently ‘universe containing’ Helium droplet alluded to earlier!

The latter major motivation for graphene research is much more down to earth and practical: Moore’s Law. Everybody knows what Moore’s Law is, and more importantly, it is becoming increasingly obvious that Moore’s Law is decelerating. Graphene’s amazing electronic and transport properties which include dissipationless transport, the strong suppression of weak localization, and width and chirality dependent band gaps and band-structures, make it a prime candidate for implementation in the next generation of electronic devices, and provide some positive contribution to extending Moore’s Law into the next few years. The outstanding questions in this area are being answered at a very rapid rate. The questions are obvious: What properties of graphene will be most useful for device application? Will disorder destroy these promising effects?

These sorts of questions form the basis for chapters 3-5 of this thesis. Chapters 3 and 4 are concerned with the optical properties of graphene based systems with different geometries. The optical response of graphene is remarkably high for a single atomic layer ($\approx 3\%$ absorption). Furthermore, the characteristic energy scales of the coupling constants often fall within the terahertz–far-infrared regimes, which are of considerable import at present. This makes the investigation of the optical properties in different geometries an obvious path to take, and some interesting results are found. Chapter 5 addresses this question of disorder, by introducing phonons into the problem. For device application, room temperature physics is of paramount importance, and so the first sensible addition to the clean system is electron-phonon interactions.

So we can see that the work contained in this thesis arises from two broad approaches to graphene research. We don’t know what the former approach will yield in the years to come, with the outstanding questions being more speculative than anything. Future progress with regard to the latter however, is quite ob-

vious: the inclusion of many types of disorder, scattering, heat, non-equilibrium approaches, exchange and correlation etc.

In any case, it is now time to explore the electronic properties of graphene more closely, in order to lay the framework for the main results of the thesis contained in chapters 2-5.